Journal of the Physical Society of Japan
Vol. 66, No. 10, October, 1997, pp. 3178-3182

Profile of Periodic Potential Modulation Probed by Magnetoresistance Oscillation of a Two-Dimensional Electron Gas

Mayumi KATO, Akira ENDO* and Yasuhiro IYE**

Institute for Solid State Physics, University of Tokyo, Tokyo 106

(Received April 25, 1997)

We have studied the profile of potential modulation introduced to a GaAs/AlGaAs heterostructure two-dimensional electron gas (2DEG) by a striped gold gate with period $a = 500$ nm on the surface. The magnetoresistance oscillation of 2DEG under one-dimensional periodic potential modulation arising from commensurability between the period and cyclotron diameter has been measured as a function of bias voltage applied to the gold gate. The bias alters both the amplitude and lineshape of the potential seen by 2DEG, with concomitant change in the magnetoresistance oscillation. The analysis of the magnetoresistance shows that with a positive bias, the modulation amplitude is considerably reduced and the third harmonic component becomes conspicuous. This suggests that the "built-in" potential modulation, caused mainly by strain resulting from differential contraction between the gold gate and GaAs, has more rectangular landscape, than the potential added by the bias. The strain-induced third harmonic component accounts for the previously unexplained extra dips in the magnetoresistance traces for a magnetically modulated 2DEG with a ferromagnetic metal gate.

KEYWORDS: potential profile, Weiss oscillation, GaAs/AlGaAs, heterostructure, two-dimensional electron gas, magnetoresistance, third harmonics

The system of microfabricated metallic gates on top of the GaAs/AlGaAs heterojunction has been widely used to confine, or to introduce potential modulation to, two-dimensional electron gas (2DEG) in the submicron lateral length scale for transport measurements in the mesoscopic systems.[1] The application of bias voltage V_g to the gates obviously modifies the electrostatic potential underneath. However, it has been recognized that potential modulation is brought about by just the presence of the metallic gates, even *without* the gate bias (V_g=0).[2-8] This "built-in" potential modulation has been attributed by theoretical calculation[9] mainly to the strain which couples to the 2DEG through the deformation potential. The strain results from the differential contraction between metallic gates and GaAs, when cooled from room temperature down to cryogenic temperature (typically 4.2 K or less) where measurements are made. For some experimental purposes, the built-in potential modulation constitutes an undesired, sometimes fatal, parasitic effect. An example for this can be found in the initial experimental attempt to observe magnetoresistance oscillation of 2DEG under periodic magnetic field modulation (magnetic Weiss oscillation).[4,6] There the effect of periodic magnetic modulation, introduced by an array of ferromagnetic metal gates, was washed out by that of native electrostatic potential modulation originating from the same gate. A technique used to circumvent the problem was to apply V_g that provides potential modulation of the opposite sign to the native one in an attempt to compensate the latter. With V_g=+500 mV, Izawa *et al.*[7] succeeded in observing the magnetic Weiss oscillation, demonstrating the usefulness of the method. In general, however, it will be difficult to achieve perfect compensation; the two types of modulation, being different in their origin, naturally manifest themselves in different lineshape in the 2DEG plane.

In the present paper, we investigate the potential landscape of the two component, the built-in potential and that added by biasing the gate, by measuring the magnetoresistance oscillation of 2DEG under one-dimensional (1D) periodic electrostatic potential modulation, arising from the commensurability between cyclotron diameter and the period (*electric* Weiss oscillation). By varying V_g applied to a periodic array of gold striped gates which introduces periodic potential to the 2DEG, the relative amplitude of the two components can be varied. This alters the profile of the potential seen by electrons in the 2DEG plane, which, in turn, can be revealed by the analysis of the magnetoresistance oscillation.

The device for the present study, schematically shown in the inset of Fig. 1 (b), was fabricated from a molecular beam epitaxy (MBE)-grown GaAs/AlGaAs single heterostructure which has as-grown electron density $n_s = 4 \times 10^{15}$ m^{-2} and mobility $\mu = 65$ m^2/(V·s) at 4.2 K. Upon the GaAs channel, 20 nm of undoped $Al_{0.33}Ga_{0.67}As$ setback, 40 nm of Si-doped $Al_{0.33}Ga_{0.67}As$ ($n_{Si} \simeq 5 \times 10^{24}$ m^{-3}) and 10 nm GaAs cap layer was grown. Therefore, 2DEG plane resides at the depth $d = 70$ nm below the surface. A standard Hall-bar was formed, and an array of gold stripes with width $a/2$ and free space $a/2$ in-between was defined by electron-beam lithography and lift-off process, where $a = 500$ nm is the period of the modulation. For the purpose of apply-

* E-mail: akrendo@kodama.issp.u-tokyo.ac.jp
** Also at: CREST, Japan Science and Technology Corporation.

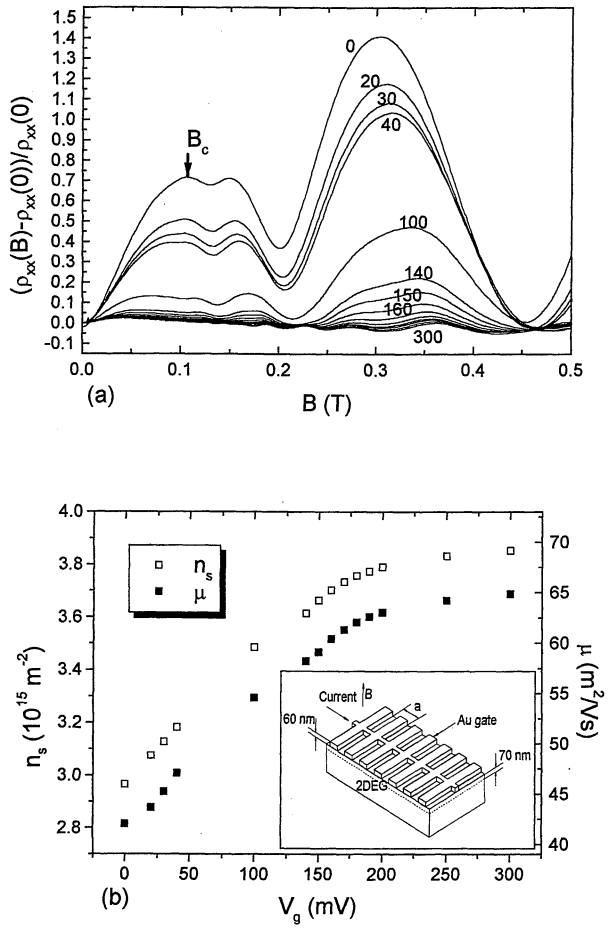

Fig. 1. (a) Magnetoresistance traces for V_g=0, 20, 30, 40, 100, 140, 150, 160, 170, 180, 190, 200, 250, 300 mV. Small numbers indicate the values of V_g (not shown for 170–250 mV). The arrow (B_c) marks the position of the maximum in the low-field positive magnetoresistance for $V_g = 0$ (see eq. (4)). (b) Dependence of (average) n_s (left axis) and μ (right axis) on V_g. Inset: Schematic illustration of the device.

ing a common bias, all the stripes are connected with a thin line of gold running parallel to the current direction, which is supposed not to disturb the measurement.

Figure 1(a) shows magnetoresistances traces for different gate biases ranging from 0 to 300 mV. The oscillatory magnetoresistance is attributed to the commensurability oscillation. As positive V_g increases, oscillation amplitude is seen to decrease drastically. This gate bias dependence tells that the built-in potential modulation has a lineshape with maxima beneath the gold stripes and minima in-between, and the applied bias ($V_g > 0$) counteracts it. The application of bias also changes the (average) electron density n_s and mobility μ as shown in Fig. 1(b) deduced from standard Hall measurments. The change in the magnetoresistance with V_g, as well as those of n_s and μ, saturates at about V_g=250–300 mV.

In Fig. 2, traces in Fig. 1 are replotted with their abscissa converted to $2R_c/a$ using the n_s, where $R_c = \hbar k_F/eB$ is the cyclotron radius with $k_F = \sqrt{2\pi n_s}$ denoting the Fermi wavenumber. The minima in resistivity ρ_{xx} (x: the direction of the current) are well established both experimentally[10,11,2] and theoretically[11-14] to appear at

$$\frac{2R_c}{a} = n - \frac{1}{4} \qquad (n = 1, 2, 3, \ldots). \tag{1}$$

For smaller V_g ($V_g \leq 100$ mV), the positions of minima agree quite well with eq. (1). For $V_g \geq 140$ mV, oscillation with another periodicity becomes conspicuous, as highlighted in the right panel of Fig. 2; additional minima appear between the original ones, and minima at $2R_c/a$= 1.75 and 2.75 turn to maxima. It is found that the positions of minima in the $V_g = 300$ mV trace are well accounted for by eq. (1) with a replaced by $a/3$ (see the top axis of the right panel in Fig. 2). It is evident that the magnetoresistance is picking up the third harmonic of the potential modulation.

The behavior outlined above is interpreted as follows.

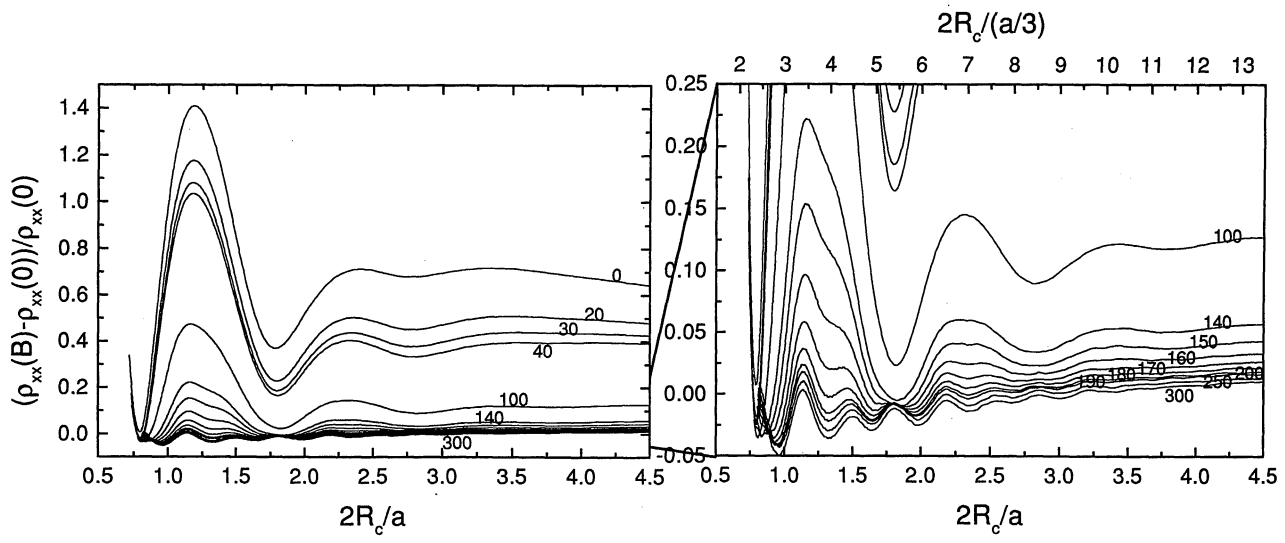

Fig. 2. Magnetoresistance traces replotted as a function of $2R_c/a$. Right panel highlights the traces for $V_g \geq 140$ mV, where the third harmonic is seen to develop.

As mentioned earlier, the potential the 2DEG sees comes from two sources; i.e., the built-in potential and the gate bias. The former is basically independent of V_g, while the latter increases with V_g. The total modulation amplitude, hence the magnetoresistance oscillation amplitude, decreases with increasing V_g, because the gate-bias-induced modulation has an opposite sign to the built-in modulation. The best compensation is realized around V_g=250−300 mV. The residual oscillatory magnetoresistance observed at those V_g reflects the difference in the lineshape of the two types of modulation. In the present case, the difference mainly consists of a third harmonic. Compared to the strong V_g dependence of the magnitude of the fundamental oscillation, the third harmonic component shows only minor change. In fact, as demonstrated below, the third harmonic component is present with roughly constant amplitude for all V_g, but becomes conspicuous when the fundamental oscillation is suppressed with large enough V_g. This suggests that the third harmonic component originates from the built-in potential modulation, and the gate-bias-induced modulation contains minimal amount of higher harmonics.

Further support of this point is obtained in Fig. 3, where the trace for $V_g = 300$ mV is subtracted from other traces with lower V_g after appropriate correction for the dependence on n_s and μ. The subtraction aims at eliminating the contribution from the third harmonic, on an assumption that at $V_g = 300$ mV the fundamental component of the potential modulation is completely compensated and that the gate-bias-induced modulation contains no third harmonic. It has been shown that the presence of two or more distinct periods produces in magnetoresistance just the superposition of oscillation curves corresponding to each period.[15,9] Smooth oscillation curves with minima at $2R_c/a = n - 1/4$ free from such dents as seen in Fig. 2 proves the validity of the assumption.

Next, we put this model to a more quantitative base to make an estimate of the amplitude of the potential modulations. By employing the expressions given by Peeters and Vasilopoulos,[13] the amplitude of the magnetoresistance oscillation for an electrostatic potential modulation $V(x) = V_0 \cos(2\pi x/a)$ is given by (for $B\mu \gg 1$)

$$(B\mu)^2 \cdot \frac{V_0}{E_F} \cdot \frac{V_0}{\hbar eB/m^*} \cdot \frac{2}{ak_F} \cdot A(T/T_a) = (\frac{V_0}{E_F})^2 \cdot (\frac{\lambda}{a})^2 \cdot \frac{2}{2R_c/a} \cdot A(T/T_a) \quad (2)$$

where $E_F = \pi\hbar^2 n_s/m^*$ is the Fermi energy, m^* the effective mass of the electron, $\lambda = \hbar k_F \mu/e$ the mean free path, and $A(x) = x/\sinh(x)$ with $k_B T_a = \hbar eBak_F/4\pi^2 m^* = E_F/(\pi^2 2R_c/a)$. We apply this formula to the $V_g = 300$ mV trace in Fig. 2, to obtain the amplitude of the third harmonic potential modulation $V_3 = 0.10$ meV. Here we replace a in eq. (2) with $a/3$ and V_0 with V_3, and use the resistance maximum and minimum at $2R_c/(a/3) \simeq 3.25$ and 2.75, respectively. Similarly, the amplitude V_1 of the fundamental component seen by the 2DEG is calculated for each V_g in Fig. 3,

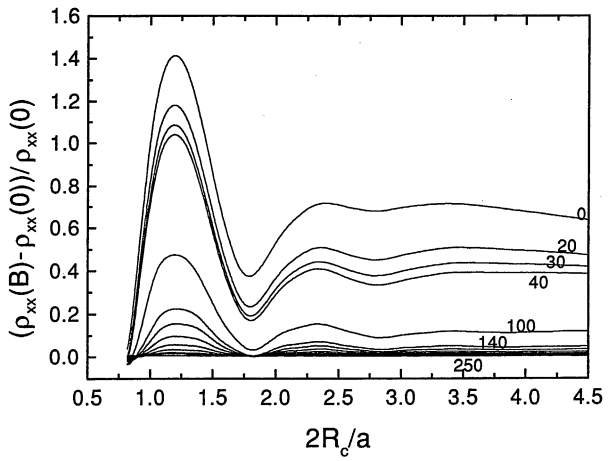

Fig. 3. The fundamental component of magnetoresitance extracted by the method explained in the text. From each trace for $0 \leq V_g \leq 250$ mV in Fig. 2, a trace of $V_g = 300$ mV multiplied by the factor $(L/E_F)^2/(L/E_F)^2_{V_g=300\text{mV}} = (\mu^2/n_s)/(\mu^2/n_s)_{V_g=300\text{mV}}$ (to correct for the dependence of the amplitude on n_s and μ, see eq. (2)) is subtracted.

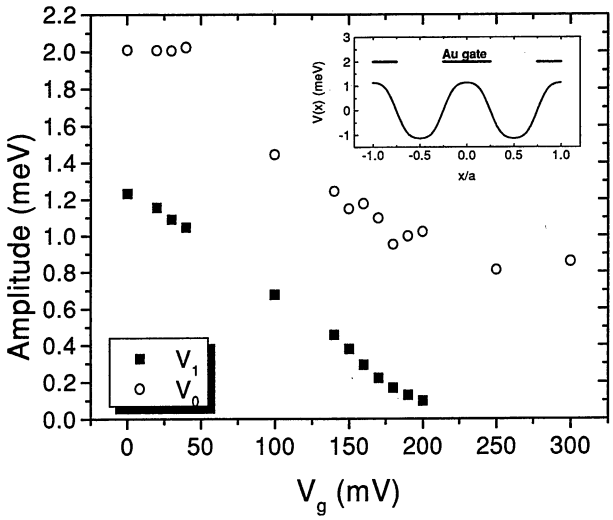

Fig. 4. Solid squares: V_1 calculated from eq. (2) using amplitude at $2R_c/a \sim 1.5$ in Fig. 3. Open circles: V_0 calculated from eq. (4) using B_c as shown in Fig. 1. Inset: Profile of the built-in potential modulation calculated by eq. (3) with V_1=1.23 meV and V_3=0.10 meV.

using the resistance maximum and minimum at $2R_c/a \simeq 1.25$ and 1.75, respectively. These are plotted in Fig. 4 by solid squares. Approximately linear dependence of V_1 on V_g is seen.

For non-zero V_g, V_1 contains (the fundamental component of) the built-in and the gate-bias-induced modulation. The former is therefore identified with V_1 at V_g=0, i.e., as[16]

$$V_{\text{built-in}}(x) = V_{1(V_g=0)} \cos(2\pi x/a) - V_3 \cos(6\pi x/a) \quad (3)$$

with $V_{1(V_g=0)} = 1.23$ mV and $V_3 = 0.10$ mV, which is depicted in the inset of Fig. 4.

The present results indicate that the built-in potential modulation has a somewhat rectangular profile while

the bias-induced electrostatic modulation is nearly sinusoidal. The latter is in accordance with the following elementary argument based on Poisson's equation. We consider a periodic potential with a general shape at $z = 0$, $V(x; z = 0) = \sum_q U_q \cos(2q\pi x/a)$. The potential profile at the 2DEG plane determined by Poisson's equation has a form $V(x; z) = \sum_q U_q \exp(-2q\pi z/a) \cos(2q\pi x/a)$. (Here we are ignoring for simplicity space charge inside the semiconductor and self-consistent contribution from 2DEG electrons themselves.) Each harmonic component falls off exponentially with z, and q-th harmonic component attenuates with a q times as short length scale as the fundamental component. Therefore although the electrostatic potential defined by the metal grating at the surface may contain substantial harmonic components, by the time it reaches the 2DEG plane, all but the fundamental component die away, leaving a nearly sinusoidal modulation there. On the other hand, strain originated at the surface is not completely relaxed even at the 2DEG plane; actually, this is why the potential modulation results.[9] Therefore the built-in potential modulation is more likely to retain higher harmonics.

Another way of estimating the modulation amplitude utilizes the positive magnetoresistance at low fields. Beton *et al.*[3] have argued that the position B_c of the maximum in the low-field positive magnetoresistance corresponds to a balancing point of the electrostatic force from the modulated potential and the Lorentzian force. For a sinusoidal potential modulation,

$$\frac{2\pi}{a} V_0 = e v_F B_c \tag{4}$$

where $v_F = \hbar k_F / m^*$ is the Fermi velocity. To generalize eq. (4) to a potential containing higher harmonics, left-hand side should be replaced with the maximum gradient of the potential. For the potential given by eq. (3), the left-hand side turns out to be $2\pi(V_1 + 3V_3)/a$. The open circles in Fig. 4 represent V_0 calculated from eq. (4) by using B_c such as the one marked by an arrow in Fig. 1 for $V_g = 0$. It is seen that V_0 is systematically larger than V_1. The gap is partly filled by taking $3V_3 = 0.30$ meV into account. A part of this discrepancy may be attributed to the ambiguity in the experimental determination of B_c. Or, the remaining difference between V_0 and $V_1 + 3V_3$ may be associated with still higher harmonics. (Note that the q-th harmonic V_q, even if small in amplitude, enters in eq. (4) with a factor q.) Considering the simplicity of our model, we take the agreement between the two sets of estimates for potential amplitude as satisfactory.

We should mention here some of the reports of harmonic Weiss oscillation by other groups. Winkler *et al.*[2] have also observed a third harmonic component in magnetoresistance oscillation under 1D periodic potential at V_g=+150, 0, and −75 mV. They deposited NiCr film onto a 2DEG wafer with periodically arranged photoresist to define periodic potential without a lift-off technique. The remaining photoresist can cause heavier strain on cooling, which may be allowing the third harmonic to appear even at negative V_g. Cuscó *et al.*[5] observed a second harmonic component instead of third with shallow (depth d=28 nm) 2DEG, to which periodic potential was introduced by an array of Au/Ti gates prepared by deposition and lift off. We have also tried similar shallow 2DEG (d=25 nm and $n_s = 4 \times 10^{15}$ m^{-2}, $\mu = 113$ m^2/(V·s) as grown) with a lifted-off nickel gate, but have not observed higher harmonics, although the modulation amplitude are larger than the similar sample with larger d owing to the nearness of 2DEG to the gate.[17] Ye *et al.*[6] have also observed higher harmonics for the $d \sim 100$ nm wafer with nickel or niobium grating. They observed the second harmonic for the sample when the width w of metal stripes equals $a/2$, while the third harmonic are observed for sample with $w = a/3$. These results are at variance with our results. Presumably, appearance or non-appearance of higher harmonics depends strongly on the specific wafer used, materials of gates,[18] details of sample preparation, or even on crystallographic orientation of the wafer with respect to the grating, which has so far been attracted little attention but can nonetheless greatly affect the strain-induced effect.[19]

The third harmonic component in built-in electrostatic potential modulation provides a good account for the extra minima unexplained so far, observed in the magnetically modulated 2DEG.[7,8] Under periodic magnetic modulation $B_m(x) = B_0 \cos(2\pi x/a)$, magnetoresitance reverses its maxima and minima compared to its electrostatic counterpart, i.e., the minima occur at

$$\frac{2R_c}{a} = n + \frac{1}{4} \qquad (n = 0, 1, 2, \ldots). \tag{5}$$

In our previous work, we used a nickel grating to generate magnetic modulation, while eliminating the potential modulation by applying +500 mV to the gate. The magnetic Weiss oscillation in agreement with eq. (5) has been observed.[7] A part of the magnetoresistance traces are reproduced in Fig. 5 with the abscissa $2R_c/a$. The up-sweep and down-sweep traces, and the difference of the two are shown. A series of resistance minima in agreement with eq. (5) are identified. Since the magnetic modulation derives from magnetization of the nickel gate, it shows hysteretic behavior. It is clear that minima seen in the difference curve originate from the magnetic modulation. However, minima indicated by the arrows conform neither to eq. (1) nor to eq. (5). Furthermore, they completely disappear in the difference curve, and therefore are irrelevant to the magnetic modulation. The origin of these dips remained unexplained at the time.[8] As shown in the top axis of Fig. 5, these dips agree with eq. (1) with a replaced with $a/3$. Therefore, these minima are attributed to the third harmonic component of the built-in electrostatic potential modulation, which do not couple with magnetic modulation since the period is different, and are unaffected by V_g since the bias-induced electrostatic modulation does not contain much of higher harmonics. Of the integers n satisfying $2R_c/(a/3) = n - 1/4$, arrows represent $n = 3p$. Those for $n = 3p - 2$ coincide with the minima of the magnetic Weiss oscillation (for $n = p - 1$ in eq. (5)). Minima expected for the third harmonic modulation at $n = 3p - 1$ are missing. Although still higher harmonics might be responsible for this, we cannot find simple explanation at present.

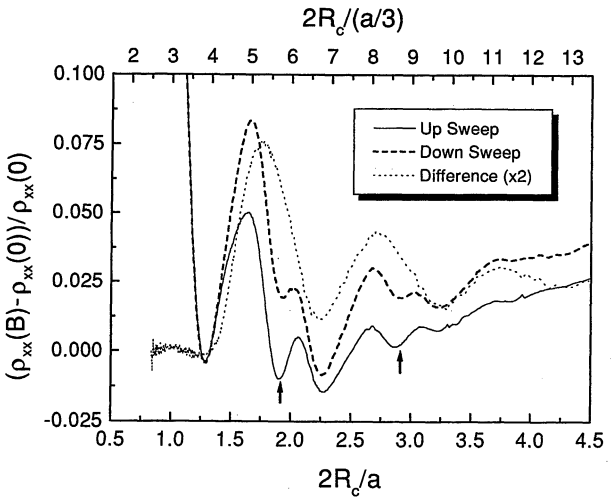

Fig. 5. Magnetoresistance traces for 2DEG with nickel grating (a = 500 nm) with V_g=+500 mV, picking up *magnetic* field modulation. Up-sweep and down-sweep, and the difference of the two (hysteretic part) are shown. Minima marked by arrows are well accounted for by the third harmonic of the built-in *electrostatic* potential modulation (see the top axis).

In summary, we have found that V_1 seen by 2DEG changes almost linearly with V_g, while V_3 is insensitive to V_g. We attribute this to the fact that the third harmonic belong to the native component of the potential modulation, which leads to the interpretation that the built-in potential is more rectangular in shape than the potential added by V_g. It is worth pointing out that at V_g = 300 mV, periodic potential with a period factor of three smaller than the fabricated length has been achieved, albeit at the cost of smaller modulation amplitude.

Acknowledgements

We would like to thank Prof. S. Katsumoto for valuable discussions. This work was supported by Grant-in Aid for Scientific Research from the Ministry of Education, Science, Sports and Culture.

1) C. W. J. Beenakker and H. van Houten: Solid State Physics, ed. H. Ehrenreich and D. Turnbull Vol. 44 p. 1.
2) R. W. Winkler, J. P. Kotthaus and K. Ploog: Phys. Rev. Lett. **62** (1989) 1177.
3) P. H. Beton, E. S. Alves, P. C. Main, L. Eaves, M. W. Dellow, M. Henini, O. H. Hughes, S. P. Beaumont and C. D. W. Wilkinson: Phys. Rev. B **42** (1990) 9229.
4) R. Yagi and Y. Iye: J. Phys. Soc. Jpn. **62** (1993) 1279.
5) R. Cuscó, M. C. Holland, J. H. Davies, I. A. Larkin, E. Skuras, A. R. Long and S. P. Beaumont: Surf. Sci. **305** (1994) 643.
6) P. D. Ye, D. Weiss, R. R. Gerhardts, K. von Klitzing, K. Eberl, H. Nickel and C. T. Foxon: Semicond. Sci. Technol. **10** (1995) 715.
7) S. Izawa, S. Katsumoto, A. Endo and Y. Iye: J. Phys. Soc. Jpn. **64** (1995) 706.
8) A. Endo, S. Izawa, S. Katsumoto and Y. Iye: Surf. Sci. **361/362** (1996) 333.
9) J. H. Davies and I. A. Larkin: Phys. Rev. b **49** (1994) 4800.
10) D. Weiss, K. von. Klitzing, K. Ploog and G. Weimann: Europhys. Lett. **8** (1989) 179.
11) R. R. Gerhardts, D. Weiss and K. von. Klitzing: Phys. Rev. Lett. **62** (1989) 1173.
12) C. Zhang and R. R. Gerhardts: Phys. Rev. B **41** (1990) 12850.
13) F. M. Peeters and P. Vasilopoulos: Phys. Rev. B **46** (1992) 4667.
14) C. W. Beenakker: Phys. Rev. Lett. **62** (1989) 2020.
15) R. R. Gerhardts: Phys. Rev. B **45** (1992) 3449.
16) Strictly speaking, relative phase θ of the fundamental and third harmonic component, $V(x) = V_1 \cos(2\pi x/a) + V_3 \cos(6\pi x/a + \theta)$ cannot be determined from magnetoresistance. However, from the symmetry of the system, θ should be either 0 or π, i.e., $V(x) = V_1 \cos(2\pi x/a) \pm V_3 \cos(6\pi x/a)$. The positive sign is discarded since it gives an unphysical triangular potential landscape.
17) M. Kato: Master Thesis, Faculty of Science, The University of Tokyo, Hongo, Tokyo, 1997 [in Japanese].
18) Dysprosium gates result in the *opposite sign* of built-in potential modulation compared to gold or nickel. See, P. D. Ye, D. Weiss, R. R. Gerhardts, M. Seeger, K. von Klitzing, K. Eberl and H. Nickel: Phys. Rev. Lett. **74** (1995) 3013.
19) P. C. Main: private communication.